

CLUSTERED STAR FORMATION IN THE SMALL MAGELLANIC CLOUD. A *SPITZER*/IRAC VIEW OF THE STAR-FORMING REGION NGC 602/N 90¹

DIMITRIOS A. GOULIERMIS, SASCHA P. QUANZ, & THOMAS HENNING
Max-Planck-Institute for Astronomy, Königstuhl 17, 69117 Heidelberg, Germany
Accepted for Publication in ApJ, May 1, 2007

ABSTRACT

We present *Spitzer*/IRAC photometry on the star-forming H II region N 90, related to the young stellar association NGC 602 in the Small Magellanic Cloud. Our photometry revealed bright mid-infrared sources, which we classify with the use of a scheme based on templates and models of red sources in the Milky Way, and criteria recently developed from the *Spitzer* Survey of the SMC (Bolatto et al. 2007) for the selection of candidate Young Stellar Objects (YSOs). We detected 57 sources in all four IRAC channels in a 6'2 × 4'8 field-of-view centered on N 90; 22 of these sources are classified as candidate YSOs. We compare the locations of these objects with the position of optical sources recently found in the same region with high-resolution HST/ACS imaging of NGC 602 by Schmalzl et al. (2007), and we find that 17 candidate YSOs have one or more optical counterparts. All of these optical sources are identified as pre-main sequence stars, indicating, thus, ongoing clustered star formation events in the region. The positions of the detected YSOs and their related PMS clusters give a clear picture of the current star formation in N 90, according to which the young stellar association photo-ionizes the surrounding interstellar medium, revealing the H II nebula, and triggering sequential star formation events mainly along the eastern and southern rims of the formed cavity of the parental molecular cloud.

Subject headings: Magellanic Clouds — HII regions — open clusters and associations: individual (NGC 602) — stars: formation — stars: pre-main sequence — Hertzsprung-Russell diagram

1. INTRODUCTION

The *Spitzer* Space Telescope opens a unique mid- and far-infrared window to the exploration of massive star formation not only in our galaxy but also in our neighboring dwarf galaxies, the Large and Small Magellanic Cloud (LMC, SMC). Stellar associations in both the Magellanic Clouds (MCs) contain the richest sample of young bright stars in these galaxies, and consequently our knowledge on their young massive stars has been collected from studies of such stellar systems (see e.g. Massey 2002). Furthermore, almost every MCs association coincide with one or more H II regions, as they have been earlier cataloged (Henize 1956; Davies et al. 1976), and it has been shown that the measured H α fluxes are in excellent agreement with those expected from the ionizing flux of the detected massive stars (Massey 1993). However, MCs associations are not mere aggregates of young bright stars alone, but they also host large numbers of faint pre-main sequence (PMS) stars, as recent HST studies showed for both the LMC (Gouliermis et al. 2006) and the SMC (Nota et al. 2006). Both, the existence of H II regions and PMS stars in stellar associations of the MCs indicate that star formation may be still active in their vicinity, and *Spitzer* offers a unique opportunity to test this hypothesis.

Indeed, using *Spitzer* observations, Jones et al. (2005) reported four Young Stellar Objects (YSOs) in the H II complex N 159 (located in the vicinity of the association LH 105; Lucke & Hodge 1970) in the LMC. Chu et al. (2005) obtained *Spitzer* observations of the super-bubble N 51D (associations LH 51/54) in the LMC and they found three YSOs projected within the super-bubble. Images from the *Hubble* Space Telescope (HST) in H α and [S II] allowed them to identify dust

globules associated with two of them. The third YSO was associated with the first Herbig-Haro object detected outside the Galaxy. Furthermore, Meixner et al. (2006) in their presentation of the first results from the *Spitzer* Space Telescope Survey of the LMC Legacy Project *Surveying the Agents of a Galaxy's Evolution* (SAGE), show as a test-case epoch 1 data of the area of two H II regions, N 79/N 83 (associations LH 2/LH 5). They found that MIPS 70 μ m and 160 μ m images of the diffuse dust emission of the regions reveal a distribution similar to the gas emissions, especially the H I 21 cm emission, and they note that the measured point-source sensitivity for the epoch 1 data is consistent with expectations for the survey.

Bolatto et al. (2007), recently, presented their results from the *Spitzer* Survey of the Small Magellanic Cloud (S³MC), which imaged the star-forming body of the SMC in all seven MIPS and IRAC wave bands. These authors compiled a photometric catalog of 400,000 mid- and far-infrared point sources in the SMC, from which they identified 282 bright candidate YSOs as bright 5.8 μ m sources with very faint optical counterparts and very red mid-infrared colors ([5.8]–[8.0] > 1.2 mag). More recently, Simon et al. (2007) used the same observations and applied spectral energy distribution (SED) fits based on models by Whitney et al. (2003a, b, 2004) to enhance the catalog of candidate YSOs in the brightest H II region in the SMC, N 66.

The present paper deals with mid-infrared imaging from the *Spitzer* Space Telescope of the H II region LHA 115-N90 (Henize 1956) or in short N 90, located in the wing of the SMC. This region, also cataloged by Davies et al. (1976) and named DEM S 166, is related to the young star cluster NGC 602, which was classified as a stellar association by Hodge (1985; system No 68 in his catalog). We present the results of our investigation on the candidate YSOs in the region of NGC 602/N 90, identified with our photometry according

Electronic address: [dgoulier], [quanz], [henning]@mpia-hd.mpg.de

¹ Research supported by the Deutsche Forschungsgemeinschaft (German Research Foundation)

The postscript file is removed due to size limitations.
To see the figure download the corresponding JPG file: “f1.jpg”

FIG. 1.— *Spitzer* image of the region surrounding NGC 602/N 90. IRAC three-color image is shown, with IRAC-1 3.6 μm in blue, IRAC-2 4.5 μm in green, and IRAC-4 8 μm in red.

to criteria based on galactic templates and recent *Spitzer* observations of other star forming regions in the SMC.

Specifically, in §2 we discuss the retrieval of the *Spitzer* data used in our study and their photometry. General description of the mid-infrared characteristics of the region is given in §3, and in §4 the point sources detected with our photometry, and the selection of candidate YSOs are presented. The recent release of high-resolution data on NGC 602/N 90 obtained with the *Advanced Camera for Surveys* on *Hubble* Space Telescope allowed us a detailed photometric study of the stellar association and its surroundings down to the faint red pre-main sequence stars of the system (Schmalzl et al. 2007). In §4 we also combine the results from both *Hubble* and *Spitzer* photometries to identify the optical counterparts of the candidate YSOs found in the region. Based on our findings we discuss the current star forming process that probably took place in the region of NGC 602/N 90 with emphasis to the clustered behavior of star formation in §5. Finally, general conclusions of this study are given in §6.

2. DATA RETRIEVAL AND PHOTOMETRY

The imaging data of our study have been obtained with the *Infrared Array Camera* (IRAC; Fazio et al. 2004) on-board *Spitzer* Space Telescope (Werner et al. 2004). The images are publicly available and are downloaded from the *Spitzer* Space Telescope Archive using the *Leopard* package². These observations (dataset archive ID: AOR 12485120) were obtained within the GTO Science Program 125 (PI: G. Fazio) on 28 November 2004. We retrieved the Post Basic Calibrated Data (pbcd) for all four IRAC channels (3.6 μm , 4.5 μm , 5.8 μm and 8.0 μm), which are already fully co-added and calibrated. After visual inspection of the images we carried out PSF-photometry with the *daophot* package provided within the IRAF³ environment. In the case of the region of NGC 602/N 90, PSF photometry is required as the field is too crowded for aperture photometry to be appropriately applied. Consequently, for each filter we constructed a reference PSF

by combining the PSF of at least 5 objects with a high signal to noise ratio and we used this PSF to fit all objects identified with a 3- σ confidence level over the local background.

We converted the pixel values in each filter from MJy sr^{-1} to DN s^{-1} according to “IRAC Data Handbook” version 5.1.1 and we computed the corresponding magnitudes as $m = -2.5 \log(f) + \Delta_{\text{ZP}}$ with f denoting the flux measured in DN s^{-1} and Δ_{ZP} being the zero point for each filter. Zero points were taken from Hartmann et al. (2005): 19.66 (3.6 μm), 18.94 (4.5 μm), 16.88 (5.8 μm) and 17.39 (8.0 μm). For the initial PSF fit we used a PSF size of 2 pixel, and applied aperture corrections as described in the “IRAC Data Handbook” to obtain the final magnitudes. Finally, we cross-matched the obtained catalogs for each filter to identify the sources that are detected in more than one IRAC bands, by allowing a maximum offset of 2 pixels for the center of each point source.

3. DESCRIPTION OF THE MID-INFRARED OBSERVATIONS OF NGC 602/N 90

Spitzer covers a suitable wavelength range (3.6 - 160 μm) for defining the dust properties of the interstellar medium (ISM). The mid-infrared channels of IRAC (3.6, 4.5, 5.8 and 8 μm) are good tracers of the smallest grains through Polycyclic Aromatic Hydrocarbon (PAH) emission. Very small grains (typical sizes 12 - 150 Å) and PAHs (typical sizes 4 - 12 Å; Desert et al. 1990) are very efficient in heating the gas through the photoelectric effect (Bakes & Tielens 1994) and therefore their analysis is very important for understanding the thermodynamics of the ISM.

IRAS data on both LMC and SMC suggest a deficit of the smallest dust grains in the low-metallicity environments of these galaxies due to the lower 12 μm emission in comparison to the Milky Way and other higher metallicity galaxies (Schwering 1989; Sauvage et al. 1990). A study in the SMC by Stanimirović et al. (2000) concluded that the dust in the SMC is dominated by large grains. The lower abundance of PAHs and very small grains in the SMC is also supported by detailed modeling of SMC UV absorption and FIR emission data by Weingartner & Draine (2001), Li & Draine (2002), and Clayton et al. (2003). A different grain size distribution with respect to the Galaxy, or grain destruction, possibly due to the intense UV radiation and/or by supernova shocks have

² Leopard can be downloaded from <http://ssc.spitzer.caltech.edu/propkit/spot/>.

³ IRAF is distributed by the National Optical Astronomy Observatories, which are operated by the Association of Universities for Research in Astronomy, Inc., under cooperative agreement with the National Science Foundation. (<http://iraf.noao.edu/>)

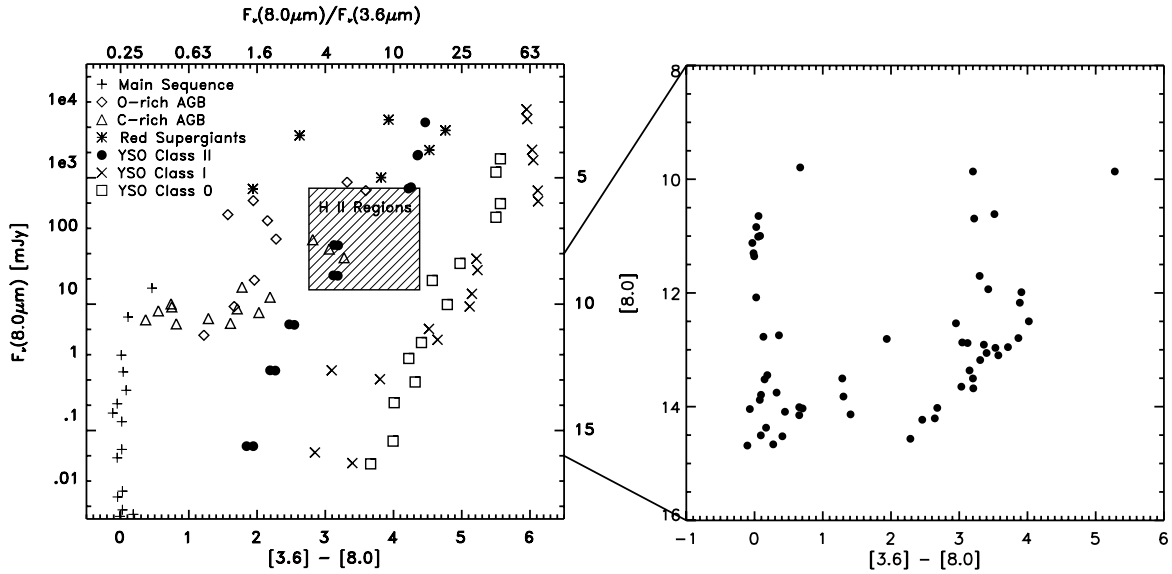


FIG. 2.— *Left*: IRAC CMD of template/model photometry of Cohen (1993) and Whitney et al. (2004) for IR sources in the Milky Way. Symbols code different types of sources throughout the SMC: Main-sequence O stars, RSGs, O-rich and C-rich AGB stars, H II regions, and YSOs. *Right*: The corresponding CMD of sources found in the region of NGC 602/N 90 with our IRAC photometry. The comparison of these CMDs denotes that there are 27 objects in our photometry (located at the right part of the CMD on the right with colors $[3.6] - [8.0] > 2$ mag) that match the type of galactic YSOs.

been proposed to explain the very small grain paucity in both galaxies. The absence of PAHs and very small grains has a profound influence on the gas heating and the existence of cold and warm phases in the interstellar medium (Wolfire et al. 1995).

The images of NGC 602/N 90 taken with *Spitzer*, which we present here, can be used for a qualitative analysis on the dust properties and its relation to stellar sources of radiation in the region of NGC 602. A color composite image from IRAC channels 1, 2 and 4 is shown in Fig. 1. The 3.6 and 4.5 μm wave-bands are mostly sensitive to stellar photospheres and very hot circumstellar dust, and therefore the blue (3.6 μm) and green colors (4.5 μm) in Fig. 1 reveal the stars, whereas the red color (8 μm) shows mainly the diffuse dust emission. Specifically, the origin of diffuse emission at 3.6 μm is likely to originate partly from bound-free transitions in the ionized gas with some contribution from the 3.29 μm emission near molecular clouds (thought to be due to C–H bond stretching in PAHs) and very small dust grain emission (e.g. Engelbracht et al. 2006). The 4.5 μm diffuse emission is a combination of bound-free continuum and Brackett- α recombination emission in H II regions. Both the 5.8 and 8.0 μm bands show molecular material in the interstellar medium (ISM) and circumstellar envelopes, as well as increasingly faint stellar photospheres. The origin of the 5.8 μm diffuse emission is most likely very warm dust emission ($T \sim 600$ K). It encompasses the 5.6 and 6.2 μm PAH band emission. The origin of the 8 μm diffuse emission is most likely the very bright emission complex at 7–9 μm thought to be dominated by C–C stretching modes (with some contribution from in-plane C–H bending) of the bonds in PAHs and very small carbonaceous dust grains (Jäger et al. 2006).

4. POINT-SOURCES DETECTED WITH SPITZER IN NGC 602/N 90

Our photometry revealed 57 objects detected in all four IRAC channels. 44 sources were identified in channels 1, 2 and 3, but not in channel 4, while only two in channels 2,3 and 4 and not in channel 1. For the classification of the sources we

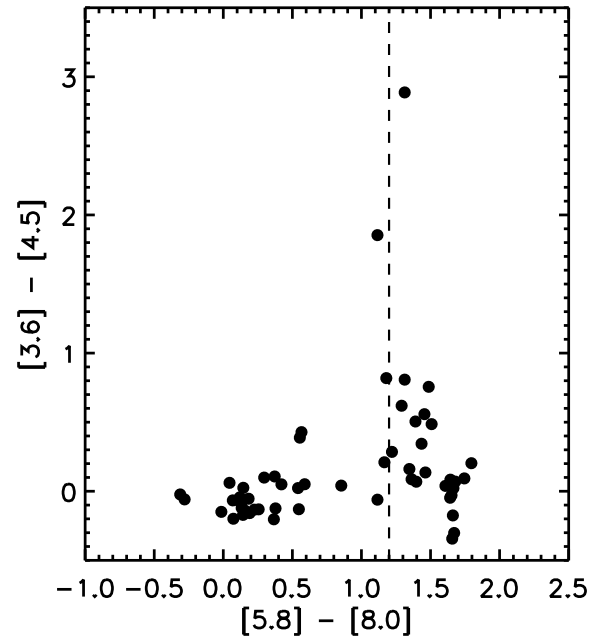


FIG. 3.— *Spitzer*/IRAC Color-color diagram of the sources detected in our photometry in the region of NGC 602/N 90. The vertical dashed line corresponds to the limit $[3.6] - [8.0] = 1.2$ mag, set by Bolatto et al. (2007) as a criterion for the selection of candidate YSOs similar to those modeled by Whitney et al. (2003). We refine our selection of candidate YSOs in the region to 22 point-sources, which are redder than this limit.

make use of the $[3.6] - [8.0]$, $[8.0]$ color-magnitude diagram (CMD) in comparison with templates and models compiled for a wide range of IR sources in the Milky Way. These templates have been developed by Cohen (1993) for IRAS data on galactic IR sources, adapted for the IRAC and 2MASS color classification scheme for the Galactic Legacy Infrared Mid-Plane Survey Extraordinaire (GLIMPSE) *Spitzer* project

The postscript file is removed due to size limitations.
To see the figure download the corresponding JPG file: “f4.jpg”

FIG. 4.— Color composite image of separate exposures made by ACS/WFC on *Hubble* Space Telescope in two broad-band filters, $F555W$ (V) and $F814W$ (I), and one narrow-band filter, $F658N$ ($H\alpha + [N II]$) of the region NGC 602/N 90. North is up and east to the left. The data of these observations are the subject of an investigation of the young stellar populations in the region (Schmalzl et al. 2007). Red boxes indicate the positions of the candidate YSOs detected with our IRAC photometry. This picture clearly indicates that current star formation takes place at the periphery of the central association NGC 602. Probably, star formation started at the association (where the highest concentration of PMS stars has been found; Schmalzl et al. 2007) and propagated outwards, mainly to the east and south, with events of ongoing clustered star formation still taking place along the dust ridges.

(Benjamin et al. 2003). We also make use of the YSO models that have been developed by Whitney et al. (2004) also for GLIMPSE. Both papers include several types of IR sources such as main-sequence stars, red giants, O-rich and C-rich AGB stars, H II regions, and YSOs. In Fig. 2 (*left*), we show the position of such sources in the $[3.6]-[8.0]$, $[8.0]$ CMD according to the templates and models. We also show the corresponding CMD for the point-sources we found in all four IRAC channels in the region of NGC 602/N 90 (Fig. 2, *right*). From the comparison of the CMDs of Fig. 2 it is shown that there are 27 objects in our photometry with positions in the $[3.6]-[8.0]$, $[8.0]$ CMD similar to galactic YSOs of class 0, I and II. However, Class 0 YSOs are very rare due to their short evolutionary phase, and such objects would be extremely faint in the IRAC bands at the distance of the SMC. Consequently, one should consider that, although few of our sources match the positions of Class 0 YSOs in the CMD according to the models, probably there are no YSOs of this class in our sample.

A criterion adopted by Bolatto et al. (2007) within the S³MC Survey (see also §1) for the selection of YSOs in their sample is based on very red $[5.8]-[8.0]$ color index (> 1.2 mag) of bright $5.8 \mu\text{m}$ sources. Support for their selection is lent by the location of these sources in the $[3.6] - [8.0]$, $[8.0]$ CMD, and the color-color diagrams in near-, mid- and far-infrared wavelengths as modeled by Whitney et al. (2003) for different objects. Bolatto et al. note that the highly reddened $8.0 \mu\text{m}$ sources occupy the region in those plots that is predicted for late Class 0 to Class II YSOs with different geometrical parameters. We further select the most probable YSOs in the region of NGC 602/N 90 by applying this criterion to the sources detected with our photometry. The $[5.8]-[8.0]$, $[3.6]-[4.5]$ color-color diagram of our sources is shown in Fig. 3 with the limit of Bolatto et al. (2007) for candidate YSOs overplotted as a vertical dashed line. There are 24 sources in our photometry that have colors $[5.8]-[8.0] > 1.2$ mag, meeting this selection criterion. All, except two of them, have been selected as candidate YSOs also according to their positions in the $[3.6]-[8.0]$, $[8.0]$ CMD (Fig. 2). Consequently, we refine the number of candidate YSOs in the region

of NGC 602/N 90 to 22 sources, which meet both criteria.

The classification scheme of Bolatto et al. predicts only $\sim 2\%$ contamination of this part of the mid-infrared color-color diagram by B stars with $24 \mu\text{m}$ emission (their Figure 12). Other types of evolved sources, such as carbon stars, RSGs and O-rich AGB stars, are located to bluer colors. In addition, Bolatto et al. estimated the contamination by background, unresolved galaxies, which can be seen throughout the SMC at infrared wavelengths. They expect 20 contaminants in their sample of 282 candidate YSOs ($\simeq 7\%$), which translates to 1.5 sources in our sample. However, detailed inspection of the candidate YSOs on the ACS image of NGC 602/N 90 revealed no suspicious background galaxies in our sample. The characteristics of the candidate YSOs revealed with our photometry in the region of NGC 602/N 90 are presented in Table 1, where we give the ID number (from our IRAC photometric catalog), the position and the magnitudes and corresponding photometric uncertainties in the four IRAC channels for each candidate YSO.

It should be noted that the classification of candidate YSOs cannot, in any case, be reduced to a single criterion, and therefore the technique described above should be considered a first-order selection. Moreover, taking into account that the selection of objects with $[5.8]-[8.0] > 1.2$ mag may compromise the actual number of YSOs, this limit should be considered a tentative one. Indeed, Allen et al. (2004) plot known stars with YSO classifications in the IRAC color-color diagram (their Fig. 4) and their Class I YSOs clearly stretch to red $[3.6]-[4.5]$ colors with $[5.8]-[8.0]$ colors less than 1.2 mag. Our selection, based on Bolatto et al. (2007) scheme, apparently causes such sources to be left out, but its use is being considered in order to reduce as much as possible the number of misidentifications. Furthermore, sources with colors $[3.6]-[4.5] \approx 0.0$ mag and $[5.8]-[8.0] > 1.2$ mag are not well represented in Whitney et al. (2003, 2004) nor in Allen et al. (2004). Based on their colors, some of them are suspected to be small H II regions, but there are no high resolution radio observations of N 90 (unlike N 159 in the LMC; Jones et al. 2005), which would provide information on the ionizing flux for these sources and help us clarify their nature.

The postscript file is removed due to size limitations.
To see the figure download the corresponding JPG file: “f5.jpg”

FIG. 5.— Color composite images constructed from our ACS observations of regions $18'' \times 18''$ wide centered on the loci where candidate YSOs have been detected. Characteristic examples of 13 candidate YSOs from Table 1 have been selected. The drawn circles, corresponding to radius $1''/2$ indicate the positions of the candidate YSOs. Blue circles denote candidate YSOs for which optical sources have been found to coincide with, while red circles the ones for which no optical sources have been identified.

TABLE 1

CANDIDATE YSOs DETECTED IN ALL FOUR IRAC CHANNELS IN THE REGION OF NGC 602/N 90. THE NUMBERING SYSTEM OF THE YSOs IS FROM OUR PHOTOMETRIC IRAC CATALOG. CELESTIAL COORDINATES ARE GIVEN IN J2000. THE MAGNITUDES OF EACH CANDIDATE YSO IN ALL CHANNELS WITH THE CORRESPONDING ERRORS ARE GIVEN IN COLUMNS 4 THROUGH 11. THE LAST FIVE COLUMNS REFER TO THE OPTICAL SOURCES FOUND WITH ACS TO FORM POSSIBLE COMPACT CLUSTERS WITHIN A RADIAL DISTANCE OF $1''/2$ AROUND EACH OF THE CANDIDATE YSOs. THE NUMBERS OF THE DETECTED OPTICAL SOURCES, THE MAGNITUDES OF THE BRIGHTEST SOURCE ($F555W_{\text{bri}}$, $F814W_{\text{bri}}$), AS WELL AS THE CUMULATIVE MAGNITUDES OF ALL STARS AROUND EACH CANDIDATE YSO ($F555W_{\text{tot}}$, $F814W_{\text{tot}}$) ARE GIVEN IN COLUMNS 13, 14, 15 AND 16 RESPECTIVELY.

ID (1)	RA (2)	DEC (3)	[3.6] (4)	\pm (5)	[4.5] (6)	\pm (7)	[5.8] (8)	\pm (9)	[8.0] (10)	\pm (11)	No (12)	$F555W_{\text{bri}}$ (13)	$F814W_{\text{bri}}$ (14)	$F555W_{\text{tot}}$ (15)	$F814W_{\text{tot}}$ (16)
1	01:29:35.66	-73:33:39.61	15.90	0.22	16.24	0.30	13.64	0.24	11.99	0.15	2	24.62	22.85	24.46	22.63
2	01:29:25.95	-73:34:46.69	16.52	0.23	16.82	0.32	14.17	0.31	12.50	0.19	5	25.45	23.62	24.66	22.45
5	01:29:26.52	-73:32:30.31	16.27	0.15	16.45	0.21	14.57	0.29	12.91	0.15	2	17.84	17.72	17.82	17.66
22	01:29:44.77	-73:33:25.31	16.46	0.21	16.50	0.26	14.70	0.32	13.06	0.17	15	23.26	21.76	21.82	20.28
24	01:29:39.23	-73:33:18.80	16.66	0.20	16.69	0.31	14.45	0.36	12.79	0.22	5	24.54	21.85	23.12	20.93
26	01:29:19.80	-73:33:12.46	16.06	0.23	16.04	0.29	13.84	0.30	12.17	0.17					
29	01:29:35.55	-73:33:30.20	14.13	0.09	14.09	0.11	12.22	0.13	10.61	0.08	8	17.49	17.30	16.73	16.65
34	01:29:23.08	-73:32:51.51	16.00	0.16	15.93	0.17	14.28	0.26	12.88	0.13	4	22.82	20.95	22.06	20.13
35	01:29:22.34	-73:32:48.17	16.67	0.27	16.60	0.36	14.63	0.35	12.95	0.22					
36	01:29:28.61	-73:34:12.14	16.88	0.31	16.80	0.42	15.32	0.50	13.68	0.29	1	25.15	24.08		
38	01:29:34.08	-73:34:11.66	16.67	0.28	16.58	0.39	14.84	0.39	13.10	0.18					
42	01:28:47.20	-73:31:31.69	16.70	0.24	16.54	0.32	15.37	0.51	14.02	0.29					
43	01:29:41.38	-73:36:24.53	15.92	0.11	15.71	0.15	14.67	0.33	12.87	0.11					
45	01:29:43.34	-73:33:43.21	16.50	0.20	16.21	0.20	14.19	0.29	12.97	0.18	2	21.90	21.22	21.89	21.16
46	01:29:30.92	-73:34:05.74	16.51	0.23	16.17	0.27	14.80	0.38	13.36	0.21	1	22.45	20.92		
49	01:29:20.44	-73:33:16.90	16.68	0.21	16.19	0.23	15.16	0.50	13.65	0.21	1	23.16	21.55		
50	01:29:37.52	-73:33:51.34	15.00	0.18	14.50	0.20	13.09	0.22	11.70	0.19	1	20.96	20.42		
51	01:29:06.45	-73:33:48.73	13.91	0.08	13.35	0.10	12.15	0.11	10.69	0.06	10	20.16	19.56	20.05	19.19
52	01:29:30.21	-73:33:10.55	15.49	0.09	14.87	0.09	13.83	0.16	12.53	0.09	1	19.30	18.62		
53	01:29:31.67	-73:34:09.39	15.36	0.14	14.60	0.13	13.42	0.17	11.94	0.07	1	26.44	24.28		
54	01:29:35.67	-73:33:02.11	13.07	0.07	12.26	0.05	11.18	0.08	9.86	0.06	9	19.34	18.54	19.29	18.42
57	01:29:35.62	-73:33:01.52	15.14	0.20	12.26	0.05	11.18	0.08	9.86	0.06	7	24.20	22.37	22.67	20.78

NOTE. — Objects No 54 and 57 being very close to each other, have been identified as distinct sources only in the $3.6 \mu\text{m}$ band. Our photometry could not resolve them in IRAC channels 2,3 and 4, and therefore they appear with the same corresponding magnitudes. Inspection of their ACS image (Fig. 5) shows indeed the existence of multiple objects very close to each other. Around each of the candidate YSOs 54 and 57 different PMS stars have been found with only four common stars. Objects No 42 and 43 are located outside the field observed by ACS, and consequently it was not possible to identify any optical sources for them.

4.1. Optical Counterparts of the Candidate YSOs

We use the results of the photometry by Schmalzl et al. (2007) on ACS/WFC imaging of NGC 602 to identify the optical counterparts of the candidate YSOs found with *Spitzer* located in this region. We cross-correlate the positions of the candidate YSOs with the ones of all stars found with ACS. For the comparison of the two catalogs we take into account the fact that the resolution provided by IRAC is almost 25

times lower than the one of WFC, and therefore the selected area around each candidate YSO to be searched for optical counterparts in most of the cases revealed more than one optical sources. Specifically, we selected a search circle with diameter of $2''/4$, which corresponds to the size of two IRAC pixels, a typical FWHM of the point-sources found with our PSF photometry. In Table 1 the results of this search are given. Specifically, in the last five columns of this table we give the number of stars from the ACS photometry, found within a ra-

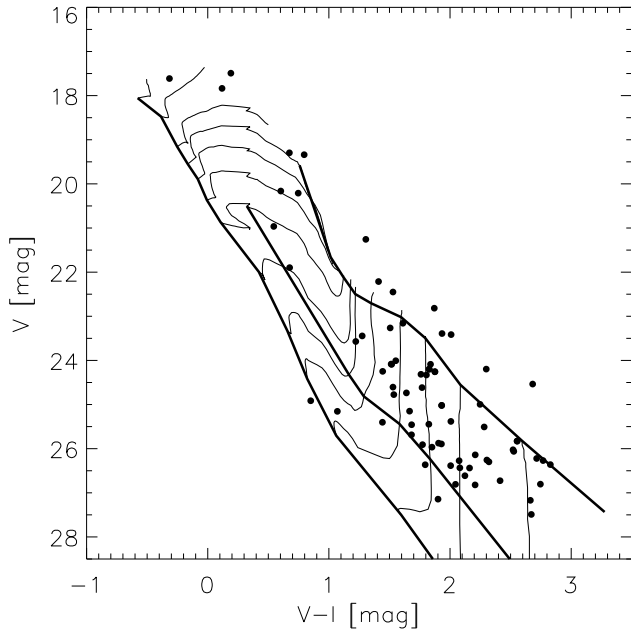


FIG. 6.— $V-I, V$ Color-Magnitude Diagram of all the optical sources from our ACS photometry, the loci of which are found to coincide (within a radial distance $1''.2$) with the location of the candidate YSOs identified with our IRAC photometry in the region of NGC 602/N 90. Evolutionary tracks for PMS stars from Palla & Stahler (1999) for masses 0.2, 0.4, 0.6, 0.8, 1.0, 1.2, 1.5, 2.0, 2.5, 3.0, 3.5, 4.0, 5.0 and $6.0 M_{\odot}$ are overplotted. This diagram shows that these optical sources are PMS stars, which cover a wide range of masses. PMS isochrone models for 0.1 and 5 Myr and the ZAMS are also plotted with thick solid lines. These models limit the age of the PMS stars, and consequently the timescale for the corresponding star formation events, to $\lesssim 5$ Myr.

dial distance of $1''.2$ (2 IRAC pixels) around the center of each candidate YSO. We also give the magnitude of the brightest optical source in the filters $F555W$ (V) and $F814W$ (I) respectively, as well as the corresponding total magnitudes from all optical sources found within the searched area around each candidate YSO. In Table 1 there are five candidate YSOs for which no optical counterpart was found. However, only three of them (No 26, 35 and 38) are located within the ACS/WFC field-of-view for which the cross-correlation was possible. The remaining two candidate YSOs (No 42 and 43) are located outside this field-of-view, since the selected area observed by IRAC (Fig. 1) is a bit larger than the one covered by ACS.

5. CURRENT STAR FORMATION IN THE AREA OF NGC 602/N 90

5.1. Clustered Star Formation Events

As shown in Table 1, almost all of the detected candidate YSOs in the area of NGC 602/N 90 are related to stars visible at optical wavelengths. In half of the cases there are more than two optical sources related to each candidate YSO (within a region corresponding to two IRAC pixels). The loci of the detected candidate YSOs are shown marked with red squares on a color composite image from the observations taken with ACS/WFC of the area of NGC 602/N 90 in Fig. 4. In this figure it is shown that there is a higher concentration of candidate YSOs to the east and south, where also the nebula is brighter and where the brighter $8\mu\text{m}$ emission is found in the *Spitzer* images (Fig. 1). More detailed color composite images from

ACS imaging of the loci around 13 selected candidate YSOs are shown in Fig. 5. Circles of radius corresponding to $1''.2$ mark the centers of the candidate YSOs. In this figure it can be seen that there are candidate YSOs coinciding with stellar clusterings, which could be true compact clusters (objects No 22, 24, 29, 54/57). The nature of these compact clusters and if they are signatures of on-going clustered star formation are two very important issues.

We attempt to address these issues by plotting the CMD of all stars from our ACS photometry, that are associated with the candidate YSOs found with IRAC. The part of a $V-I, V$ CMD, which is expected to be occupied by pre-main sequence (PMS) stars of star-forming regions in the MCs observed with *Hubble* is fairly known (e.g. Gouliermis et al. 2006, Nota et al. 2006). This CMD for the optical sources related to the candidate YSOs in the region of NGC 602/N 90, plotted in Fig. 6, shows that all of the stars found to coincide with the candidate YSOs in our sample are actually PMS stars, suggesting that either we probably observe the existence of compact PMS star clusters recently formed (or currently under formation) around typical YSOs, or that the sources identified as candidate YSOs are themselves unresolved young PMS clusters. In either case it is almost certain that these stellar concentrations demonstrate possible events of extragalactic clustered star formation on the act. If so, it would be interesting to know how long ago this formation took place.

To answer this question, on the CMD of Fig. 6 we also plot PMS evolutionary tracks from the models by Palla & Stahler (1999), and two indicative isochrones (for 0.1 and 5 Myr) and the Zero Age Main Sequence (ZAMS) from the same models. Simulations of the positions at the $V-I, V$ CMD of all PMS stars found in the region of NGC 602/N 90 by Schmalzl et al. (2007) indicate that reddening, variability and binarity are important factors, which cause a spread of the loci of PMS stars in this CMD and that even modest interstellar reddening (Schmalzl et al. find $E(B-V) \simeq 0.04 - 0.06$ mag for the association NGC 602) can make these stars appear younger (being “pushed” to redder colors). Considering these results and the plot of Fig. 6, one may conclude that the PMS stars, which coincide with the candidate YSOs of our sample do not seem to be older than about 5 Myr, giving an upper limit to the time-scale within which these clusters were formed.

For a more detailed analysis one should concentrate on the stellar content of each of the individual clusters, but in most of the cases very low numbers of stars per cluster do not allow such an analysis. We selected the most populous among the identified clusters (the ones corresponding to candidate YSOs No 22, 29, 51 and 54) to plot their individual CMDs, but the stellar numbers were still not enough to define a more narrow age range. PMS stars are mainly red sources, and therefore near-infrared imaging with cameras equipped with Adaptive Optics (AO) systems would provide the necessary resolution for a richer sample of PMS stellar members in these clusters. Indeed, high resolution near-infrared observations of these clusters would certainly be very useful, because they would 1) provide better statistics with higher numbers of detected members, enough to plot the CMDs of individual clusters and 2) fill the gap between optical and mid-infrared wavelengths, providing near-infrared magnitudes for these PMS stars. The later information will offer the opportunity to construct accurate spectral energy distributions (SEDs) of candidate YSOs, to be compared to models.

As far as candidate YSOs that coincide with no more than two PMS stars concerns, in Fig. 5 we also show several dif-

ferent cases of “single” candidate YSOs (e.g. objects No 1, 5, 49, 53), but as their images show it is unclear if such sources are indeed single isolated objects or embedded clusters (as the faint magnitudes given in Table 1 suggest), or even one massive embedded protostar. Modeling of the SEDs of such objects is quite difficult, in the sense that many different models seem to fit the SEDs, due to their small number of points, and near-infrared AO observations would certainly add three more points to the SEDs, throwing more light toward this direction as well. It is worth noting that Fig. 5 also demonstrates few interesting cases of candidate YSOs (objects No 26, 49, 34, 35, 46 and 53), both with and without optical counterparts, which are located at the edge of features similar to the “Pillars of Creation” or “Elephant Trunks” in the galactic H II region M 16 (the Eagle Nebula; Hester et al. 1996).

5.2. Star-Formation Scenario for the Region of NGC 602/N 90

The sample of candidate YSOs derived from our IRAC photometry in the region of NGC 602/N 90 (Table 1) is based on a single classification scheme. As a consequence, although it is almost certain that this sample does include true YSOs, there is always a possibility that it also includes sources misidentified as YSOs, like small H II regions, or that it is quite incomplete not including all possible true YSOs, like the Class I YSOs in the sample of Allen et al. (2004). The identification of PMS stars in the areas of the candidate YSOs as their optical counterparts indicates that half of these objects are not single sources. But, considering the difficulty of modeling the SEDs of these objects, it is not straightforward to clarify which of them represent embedded proto-clusters. In the case of candidate YSOs coinciding with one or two PMS stars, there is no information if there should be more optical counterparts, which simply were not detected in our ACS photometry, or if these are indeed single proto-stellar objects.

In any case, the composite ACS image of the area of NGC 602/N 90 shown in Fig. 4 provides evidence that sequential star formation does take place in the area and especially on the dust ridges of a cavity, which seems to extend outwards. This feature is most probably the product of photoionization by the young association, NGC 602, located almost at its center. The combination of both ACS (Fig. 4) and IRAC (Fig. 1) observations provides a more complete image of the star formation in the area. Specifically, taking into account the loci of the sources classified as candidate YSOs, the ISM features shown in the image from ACS, and the 8 μm emission shown in the IRAC image, one may conclude that in the observed area the stellar association NGC 602 ionizes the surrounding material giving birth to the H II region, N 90, and producing a cavity in the remaining of its parental molecular cloud. This event triggers sequential star formation not later than ~ 5 Myr ago, which seems to propagate mostly to the east and south. This second star formation event may be characterized by higher a concentration of YSOs, most of which may be related to compact PMS clusters. This scenario is also supported by the study of the PMS population in NGC 602 and its surroundings by Schmalzl et al. (2007).

6. CONCLUSIONS

We present our results from *Spitzer*/IRAC photometry on the star-forming region NGC 602/N 90 in the Small Magellanic Cloud.

We performed PSF photometry on IRAC images taken in four mid-infrared channels (3.6 μm , 4.5 μm , 5.8 μm and 8.0

μm) centered on the H II region N 90. We identified 57 objects in all four channels and 44 in channels 1, 2 and 3. We classified the sources found in all four IRAC channels from their loci in the [3.6]–[8.0], [8.0] color-magnitude diagram, based on templates and models for different red sources in the Milky Way, and the [5.8]–[8.0], [3.6]–[4.5] color-color diagram, according to the classification scheme developed by Bolatto et al. (2007) for SMC YSOs.

According to our classification there are 22 candidate YSOs in the region of NGC 602/N 90. We use our results from PSF photometry in the filters *V* and *I* of the same region from imaging with the Wide-Field Channel of ACS on-board the *Hubble* Space Telescope (Schmalzl et al. 2007) to identify optical sources, which coincide with the candidate YSOs. All these optical sources are identified as PMS stars. We found that almost half of the candidate YSOs match with no more than two PMS stars, but examination of their loci on the ACS images does not exclude the possibility that there may be more highly embedded sources or not well resolved also in the optical. The remaining candidate YSOs coincide with more than 3 PMS stars, and four of them seem to include small compact PMS clusters of 7 (or more) stars. We found that these stars are probably formed earlier than 5 Myr ago, according to PMS evolutionary models. We could not find any optical counterpart for five YSOs, two of which are located outside the field observed with ACS.

From the positions of the detected candidate YSOs, we conclude that they are probably the products of a sequential star formation process, which presumably propagates mostly to the east and south, on the ridges of the molecular cloud, as they formed from the photo-ionizing process of the stellar association NGC 602 located in the center of the apparent cavity of the cloud.

Finally, it should be mentioned that our sample of candidate YSOs may be contaminated by other objects like small H II regions, or it may not include some true YSOs. Based on our results we stress the importance of high-resolution near-infrared imaging of the candidate YSOs in order 1) to resolve more faint red stellar sources and detect a higher number of related PMS stars, and 2) to fill the wavelength gap between optical and mid-infrared by providing near-infrared measurements of all detected sources, so that their SEDs will be thoroughly modeled, as well as of high-resolution radio observations, which will provide additional information on the ionizing flux for the identified objects.

Dimitrios A. Gouliermis kindly acknowledges the support of the German Research Foundation (Deutsche Forschungsgemeinschaft - DFG) through the individual grant 1659/1-1. Sascha P. Quanz kindly acknowledges financial support from the German Friedrich-Ebert-Stiftung. This paper is based on observations made with the *Spitzer* Space Telescope, which is operated by the Jet Propulsion Laboratory, California Institute of Technology under a contract with NASA, and on observations made with the NASA/ESA *Hubble* Space Telescope, obtained from the data archive at the Space Telescope Science Institute. STScI is operated by the Association of Universities for Research in Astronomy, Inc. under NASA contract NAS 5-26555. This research has made use of NASA’s Astrophysics Data System, *Aladin* (Bonnarel et al. 2000), *WCSTools* (Mink 2001), and the SIMBAD database, operated at CDS, Strasbourg, France.

REFERENCES

- Allen, L. E., et al. 2004, *ApJS*, 154, 363
Bakes, E., & Tielens, A. G. G. M. 1994, *ApJ*, 427, 822
Benjamin, R. A., et al. 2003, *PASP*, 115, 953
Bolatto, A. D., et al. 2007, *ApJ*, 655, 212
Bonnarel, F., et al. 2000, *A&AS*, 143, 33
Clayton, G. C., Wolff, M. J., Sofia, U. J., Gordon, K. D., & Misselt, K. A. 2003, *ApJ*, 588, 871
Cohen, M. 1993, *AJ*, 105, 1860
Davies, R. D., Elliott, K. H., & Meaburn, J. 1976, *MmRAS*, 81, 89
Desert, F.-X., Boulanger, F., & Puget, J. L. 1990, *A&A*, 237, 215
Engelbracht, C. W., et al. 2006, *ApJ*, 642, L127
Fazio, G., et al. 2004, *ApJS*, 154, 10
Gouliermis, D., Brandner, W., & Henning, T. 2006, *ApJ*, 636, L133
Hartmann, L., et al. 2005, *ApJ*, 629, 881
Henize, K. G. 1956, *ApJS*, 2, 315
Hester, J. J., et al. 1996, *AJ*, 111, 2349
Jäger, C., Krasnokutski, S., Staicu, A., Huisken, F., Mutschke, H., Henning, T., Poppitz, W., & Voicu, I. 2006, *ApJS*, 166, 557
Jones, T. J., Woodward, C. E., Boyer, M. L., Gehrz, R. D., & Polomski, E. 2005, *ApJ*, 620, 731
Hodge, P. 1985, *PASP*, 97, 530
Li, A., & Draine, B. T. 2002, *ApJ*, 576, 762
Massey, P. 1993, *Massive Stars: Their Lives in the Interstellar Medium*, 35, 168
Massey, P. 2002, *ApJS*, 141, 81
Mink, D. J. 2002, *ASP Conf. Ser. 281: Astronomical Data Analysis Software and Systems XI*, 281, 169
Palla, F., & Stahler, S. W. 1999, *ApJ*, 525, 772
Sauvage, M., Vigroux, L., & Thuan, T. X. 1990, *A&A*, 237, 296
Schwering, P. B. W. 1989, *A&AS*, 79, 105
Simon, J. D., et al. 2007, submitted to *ApJ*
Schmalzl, M. et al. 2007, to be submitted to *ApJ*
Stanimirović, S., Staveley-Smith, L., van der Hulst, J. M., Bontekoe, T. R., Kester, D. J. M., & Jones, P. A. 2000, *MNRAS*, 315, 791
Weingartner, J. C., & Draine, B. T. 2001, *ApJ*, 548, 296
Werner, M., et al. 2004, *ApJS*, 154, 1
Whitney, B. A., Wood, K., Bjorkman, J. E., & Cohen, M. 2003, *ApJ*, 598, 1079
Whitney, B., Indebetouw, R., Bjorkman, J. E., & Wood, K. 2004, *ApJ*, 617, 1177
Wolfire, M., Hollenbach, D., McKee, C. F., Tielens, A. G. G. M., & Bakes, E. L. O. 1995, *ApJ*, 443, 152

This figure "f1.jpg" is available in "jpg" format from:

<http://arxiv.org/ps/0705.3359v1>

This figure "f4.jpg" is available in "jpg" format from:

<http://arxiv.org/ps/0705.3359v1>

This figure "f5.jpg" is available in "jpg" format from:

<http://arxiv.org/ps/0705.3359v1>